Proceedings World Geothermal Congress 2026
Calgary, Canada, June 8 – 11, 2026

Stress, Slip, and Productivity: Integrated Geomechanical Modeling of the Þeistareykir Geothermal Reservoir – Part 2 Reservoir-Scale

Drew L. Siler[1]*, Irene C. Wallis[2], Guðjón Helgi Eggertsson[3]^, and Anette Kærgaard Mortensen3
Geologica Geothermal Group[1]*, Cubic Earth[2], and Landsvirkjun3, now at Baseload Capital^
dsiler@geologica.net

Keywords: Faults, accommodation zone, permeability, structural control, stress, strain, stress rotation

ABSTRACT

We present an innovative multi-scale geomechanics analysis of Þeistareykir geothermal field, Iceland. Results are consistent across scales and are a good match to the distribution of reservoir productivity. Þeistareykir is a high temperature (~350°C), volcanic-hosted, two-phase geothermal system with 90 MWe of installed capacity. It is localized by an accommodation zone that consists of west-dipping normal faults to the north and east-dipping normal faults to the south. The reservoir-scale analysis, presented herein, focuses on static and dynamic geomechanical modelling of reservoir-scale faults. The wellbore-scale analysis, presented in a companion paper (Wallis et al. 2026), focuses on integration of borehole image data to parameterize stress tensor models and reveal the wellbore-scale geologic controls on permeability.

Reservoir-scale static geomechanical analysis indicates that the rift zone-parallel (north to north-northeast striking) normal faults, which dip ~75° east and west, are best oriented to control permeability. This result is consistent with the wellbore-scale work. The dynamic modeling determines slip induced by the local stress regime, and the stress and strain effects of that modeled slip. Modeling results show relatively long and narrow permeability 'sweet spot' on the western side of the field. This area is coincident with the accommodation zone and includes the most productive wells. Dynamic modelling also reveals slip-induced counter-clockwise stress rotations at the reservoir-scale. These are co-located with similar stress rotations revealed by drilling induced damage in borehole image logs, some of which were coincident with large feed zones. This finding links the wellbore-scale results, reservoir-scale results, and productive permeability and highlights the key innovation of this study.

1 INTRODUCTION

Þeistareykir is a high temperature (~350°C), volcanic-hosted, two-phase geothermal system with 90 MWe of installed capacity located in the Northern Rift Zone of Iceland (Figure 1). Rift parallel (north-to-north-northeast striking) faults and fissures mapped at the surface in the Þeistareykir area suggest a prominent rift parallel structural control to permeability in the geothermal reservoir. However, Þeistareykir also lies on the southern edge of the Húsavík-Flatey fault zone, a system of west-northwest-striking, right-lateral strike-slip faults (Bergerat et al., 2000). The Þeistareykir geothermal field is beneath and adjacent to Bæjarfjall Mountain (Figure 1), a tuya or hyaloclastite mountain interpreted as marking the volcanic center of the Þeistareykir volcanic system (Magnúsdóttir and Brandsdóttir, 2011). It is unclear what role each of the three different structural zones, the rift-parallel, north-northwest-striking faults, west-northwest-striking fault system, or the structure of the volcanic center play in controlling permeability in the Þeistareykir geothermal reservoir. This paper presents the reservoir-scale portion of a novel, multi-scale geomechanical analysis conducted to inform on this question of reservoir permeability. A companion paper addresses the same permeability question at the wellbore-scale.

2 DATA AND METHODOLOGY

An extensive geological dataset exists for Þeistareykir. This includes both published and proprietary Landsvirkjun geological maps (Sæmundsson, 2007, Sæmundsson et al., 2012), fault maps (Khodayar and Björnsson, 2018, Khodayar et al., 2018), and structural geology/tectonics studies (e.g., Blischke, et al., 2022, Tibaldi et al., 2020, Þorsteinsdóttir et al., 2019). Additionally, a 3D geological model containing some 110+ 3D dimensional fault planes was made available for geological and structural characterization in this study. Several dozen vertical and inclined geothermal wells have been drilled at Þeistareykir (Figure 1). Data from these wells analyzed herein include lithologic, structural, temperature, pressure, steam flow rate, and injectivity index.

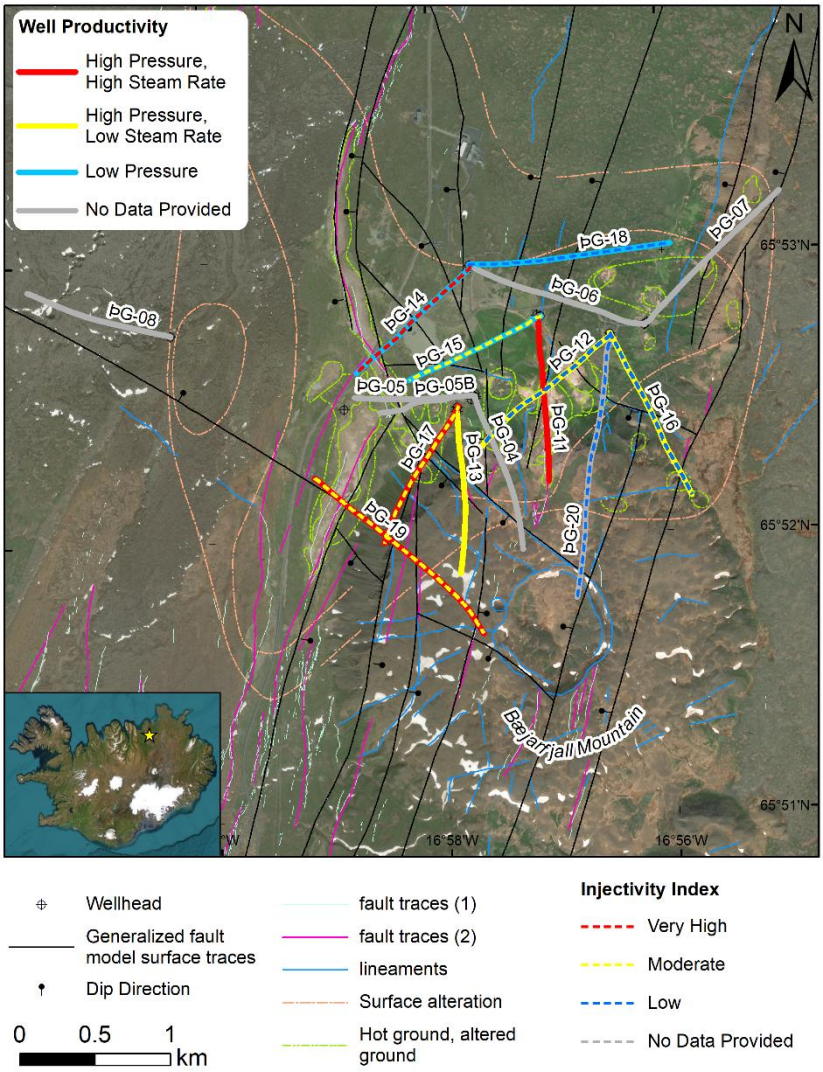


Figure 1. Map of Þeistareykir geothermal field, inset shows location in Iceland. Wells are classified by pressure and steam flow rate (solid line well paths) and injectivity index (dash well paths). Surface fault traces shown are from the generalized fault model built as part of this work

2.1 Fault Data

As explained above, there is an extensive structural data set at Þeistareykir. For the analysis herein, the structural model needed to be simplified and generalized such that the numerical calculation was tractable, yet still representative of the structural complexity characterized through surface fault mapping, image log interpretation, and 3D structural modeling. The generalization of the structural model was accomplished by comparing all existing datasets, identifying the key structural trends present in all data sets, and selecting the major structures with well-characterized geometry in all or most existing datasets.

This process of generalizing the structural model, which is necessary for the numerical calculations, also commonly reveals key 'big picture' aspects of the fault structure and allows one to see the forest through the trees, so to speak. In this case, the analysis which yielded the generalized structural model revealed two critical characteristics about the fault structure at Þeistareykir. First and foremost, it is clear that an accommodation zone (Figures 1 and 2a), characterized by east-dipping faults to the south and west-dipping faults to the north, occurs at the northwest corner of Bæjarfjall Mountain (e.g. Tibaldi et al., 2020) coincident with many of the geothermal production wells. Secondly, the fault dips in the 3D geological model, and therefore the generalized fault model as well, are more steeply dipping than the fault and fracture dips as characterized in the borehole image (BHI) logs (Figure 2b).

The simplified fault model consists of twenty-two (22) faults (Figure 1). Four (4) NNW-striking east-dipping normal faults, cutting through and to the south of Bæjarfjall, and seven (7) NNW-striking west-dipping normal

faults to the north of Bæjarfjall constitute the accommodation zone. Wellbore-scale (Wallis et al., 2026, this volume) and reservoir-scale static stress modeling indicate that these NNW-striking (rift parallel) faults are most advantageously oriented for fluid flow. There are also several west-northwest-striking faults sub-parallel to the trend of the Húsavík-Flatey fault zone. The faults that constitute the generalized fault model are steeply dipping, 80-90°. These fault dips are sourced from the 3D geologic model and represent a narrower range of dip than the BHI data. The decision to retain the steep dips from the 3D geologic model was made for continuity between this work and existing reservoir characterization. The inconsistency between the range of dips in the generalized fault model and the range dips seen in the BHI data (Wallis et al., 2026, this volume) are one area where this study could be potentially improved.

2.2 Stress Data

A new stress model was built based on re-analysis BHI data (Wallis et al., 2026, this volume). Of the eleven wells reviewed, three were selected for detailed re-interpretation and wellbore-scale geomechanical modelling: ÞG-14, ÞG-16, and ÞG-19 (Figure 1). These wells were chosen based on their locations (they approximately span the wellfield N/S and E/W), as well as the quality of the BHI data and its appropriateness for stress modelling. As is common for BHI acquired in thermally stressed, volcanic-hosted geothermal wells, the morphology of the drilling induced damage is complex and prevented modelling the magnitude of SHmax. Instead, 1D Stress scenarios ranging from normal to transitional to strike-slip faulting stress regime are an acceptable fit to the drilling induced damage data in each of the three wells. The reader is directed to Wallis et al., (2026, this volume) for detailed 1D stress modeling results. Sensitivity analyses suggested that the reservoir-scale dynamic modeling results were not particularly sensitive to variations in stress regime (i.e., normal, transitional, or strike-slip). As a result, we focus on results calculated using the transitional stress regime stress model herein.

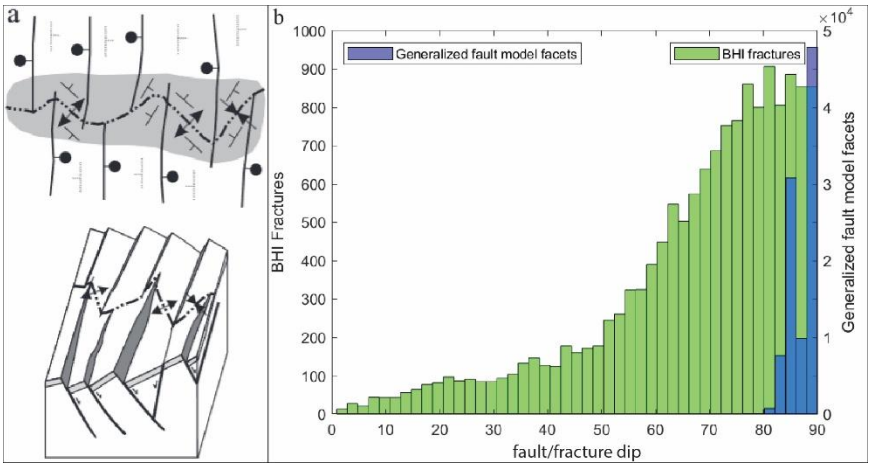


Figure 2. a) Conceptual cartoon of an accommodation zone from Faulds and Varga, 1998. b) Histogram of faults and fracture dip from the generalized fault model (blue) and BHI (green).

Table 1. 1D stress values for the three wells used in this study. These values were linearly interpolated in 3D space to construct a continuous 3D stress model for the dynamic modeling.

	Pore pressure (Mpa)	Vertical stress (Sv) magnitude (Mpa)	Maximum horizontal stress (SHmax) magnitude (Mpa)	Maximum horizontal stress (SHmax) azimuth	Minimum horizontal stress (Shmin) magnitude (Mpa)	Minimum horizontal stress (Shmin) azimuth
ÞG-14	16	43.2	43.2	168°	24.7	78°
ÞG-16	16.1	44.5	44.5	174.5°	25.2	84.5°
ÞG-19	17.0	49.0	49.0	184°	27.3	94°

A spatially continuous 3D stress model constrained by 1D stress modeling in ÞG-14, ÞG-16, and ÞG-19 was interpolated for the model domain, which spans 4 km x 4 km centered on the well field. It included pore-pressure, vertical stress (Sv), maximum horizontal stress (SHmax) magnitude and direction, and minimum horizontal stress (Shmin) magnitude and direction. Table 1 shows the stress magnitudes and directions at -1500 m asl (~2100 m depth), approximately reservoir depth. Though the stress magnitudes are relatively uniform, spatially there is an ~16° counter clockwise rotation of the direction of the principal stresses from south to north across the field (Table 1).

2.3 Lithologic data

The reservoir scale stratigraphic framework at Þeistareykir was analyzed to evaluate whether there is a lithologic control, in addition to a structural control on permeability. The detailed lithologic characterization was generalized by rock type and composition and compared to ABI caliper and acoustic amplitude data from wells. A generalized mechanical stratigraphy (i.e., soft, medium, hard) was built from these data. The 'soft' rocks consist of relatively shallower formations of hyaloclastite, pillow lavas, and interbedded basaltic lava flows, whereas the 'hard' rocks consist of relatively deep basaltic lava flows and silicic intrusive rocks. The 'medium' mechanical stratigraphic unit represents a transitional zone between these two end members. This mechanical stratigraphy was compared to the location and relative size of feed zones in wells (Figure 3).

2.4 Dynamic Stress Modeling

Our study is focused on characterizing the controls on fracture permeability at Þeistareykir. For the methodology employed in this study (modified after Siler, 2023), we assume that the major faults in the Þeistareykir area, i.e., the generalized fault model, slip periodically as a result of tectonic extension and crustal construction (e.g., dike intrusions, faulting, and eruptions) occurring in Iceland's Northern Rift Zone. Over many slip or rifting cycles, repeated slip on the major faults will cause similar and repeated stress and strain effects on the surrounding crust. These repeated stress and strain effects result in generation and maintenance of permeability in the same locations relative to the major faults. We infer that this constant generation and re-generation of fracture permeability allows the geothermal fluid flow pathways to remain open to flow despite the destruction of permeability caused by hydrothermal mineralization. The induced stress and strain effects are calculated on a 50 m discretized grid throughout the model domain. Figures 4 and 5 show results of the discretized grid interpolated throughout the model domain.

The analytical workflow proceeds in the following steps:

1) Displacement (fault slip) caused by the extant stress regime (see 2.2 Stress Data above) on the 22 faults that constitute the generalized 3D structural model is calculated. The dip-slip, strike-slip, and opening mode displacement are calculated for each triangular fault facet.

2) The changes from the initial stress state brought on by the model slip are calculated. The new, slip-affected magnitudes and directions of the principal stresses are calculated for each cell in the boundary element model domain.

3) The dilatational strain and shortening brought on by the modeled slip are calculated for each cell in the model domain.

4) The resolved stress (traction) changes on fractures throughout the model domain caused by the modeled slip are calculated. We assume that the mapped faults and the natural fractures picked in the BHI together are representative of the smaller-scale fracture fabric throughout the model domain. For each model cell, the stress changes on fractures of all orientations within ± 1 standard deviation of the orientations of the input faults and BHI fractures are calculated. At Þeistareykir this means that resolved stress (traction) changes are calculated for all possible combinations of N-to-NE-striking west- and east-dipping and WNW-to-NW-striking north- and south-dipping fractures with dips ranging from 50-90° (Figure 2b) in each cell. For each cell, the maximum (either positive or negative) traction change for all possible combinations of strike/dip is analyzed.

The slip, stress changes, strain, and traction changes are calculated in 3D dimensions throughout the model domain; ~4km x 4km centered on the well field and from the surface to -2500 m asl. Herein for ease of illustrating the key observations of the model results, we display the results as horizontal slices at reservoir depth, -1500 m asl

3 RESULTS

Our results indicate that there are two key controls on reservoir-scale productive permeability at Þeistareykir, lithologic and structural. The reservoir-scale lithological control on permeability is influenced by the mechanically 'hard' rock types and the presence of silicic intrusive rocks (Figure 3). The structural control on permeability is dependent on the accommodation zone along the western side of the well field. Dynamic modeling indicates that the accommodation zone localizes stress rotations, increases in differential stress, dilation, and increases in shear traction on faults. Each of these changes increases the likelihood of fault slip, and permeability generation/maintenance.

3.1 Lithologic Control

We constructed a mechanical stratigraphy at Þeistareykir using the ABI caliper, acoustic amplitude, and lithologic descriptions of drill cuttings. The 'soft' mechanical unit is generally defined by hyaloclastite-dominated lithologies, low acoustic amplitude, and borehole oversizing. The 'medium' unit consists of mostly basaltic lavas below the hyaloclastites. The 'medium' unit has less significant borehole size variation and low to moderate acoustic amplitude. The 'hard' unit has very uniform bore hole size and commonly has high acoustic amplitude. The 'hard' unit correlates with basaltic lavas and, importantly, acidic (or silicic) intrusive rocks in many wells.

Wells ÞG-11 through ÞG-20 have few shallow feed zones in the 'soft' formations and these tend to be smaller. Larger feed zones are more common in the 'medium' and 'hard' rocks, including the more silicic types. In the north-eastern wells (ÞG-12, ÞG-11, ÞG-16, and ÞG-18), most large feed zones are hosted within 'hard' basaltic formations. Silicic intrusive rocks are most prevalent in the four southwestern-most wells (ÞG-19, ÞG-17, ÞG-13, and ÞG-20). The silicic formations, along with the 'hard' basaltic formations tend to host large and medium feed zones in these wells (Figure 2). From this we infer that the mechanically harder rock types are more favorable for fault/fracture generated fluid flux. The reasons are twofold: (1) the medium and hard rock types are more prone to brittle failure whereas stress applied to a soft rock may be accommodated by partial/clast rearrangement or ductile deformation and (2) asperities and/or fracture rugosity/sinuosity in a hard rock can prop open fractures and assist with sustaining volume/aperture over time.

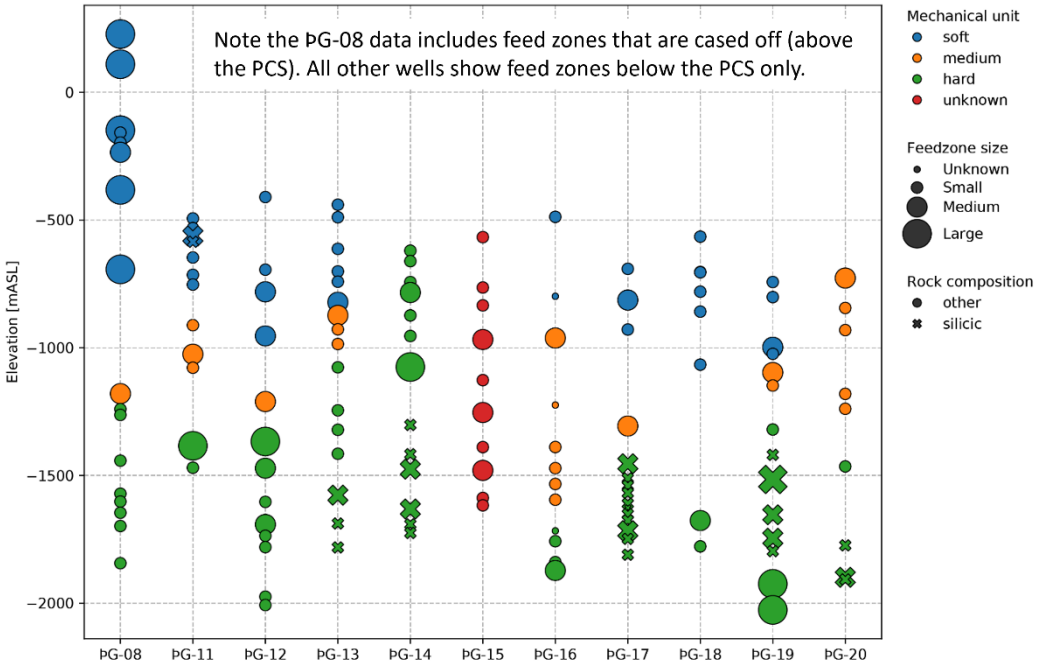


Figure 3. Mechanical stratigraphy, rock type, and feed zone size in Þeistareykir wells. Most large and medium feed zones occur and 'hard' and silicic formations.

3.2 Structural Control

3.2.1 Stress Rotations

Analysis of drilling induced damage from BHI data in wells ÞG-14, ÞG-16, and ÞG-19 document counter-clockwise vertical axis stress rotations (rotations in SHmax) in all three wells at reservoir depth, ~2000-2800 mMD. These rotations are ~7-10° (ÞG-14), ~3° (ÞG-16), and 14-22° (ÞG-19). ÞG-14 and ÞG-19 have medium and

large feed zones within the rotated interval and ÞG-16 has one medium and several small feed zones in the rotated interval. This suggests that local stress rotation in these parts of the field may be a key control on the occurrence of feed zones in these wells. See Wallis et al., (2026, this volume) for a more detailed description of these results.

The dynamic modeling results show that fault slip causes counter-clockwise rotations in the direction of SHmax in all three wells at reservoir depth (Figure 4a). This agreement between independent datasets at the wellbore-scale (BHI results) and the reservoir-scale (dynamic modeling results) provides a key validation that this analysis provides internally consistent results regarding productive permeability across multiple scales.

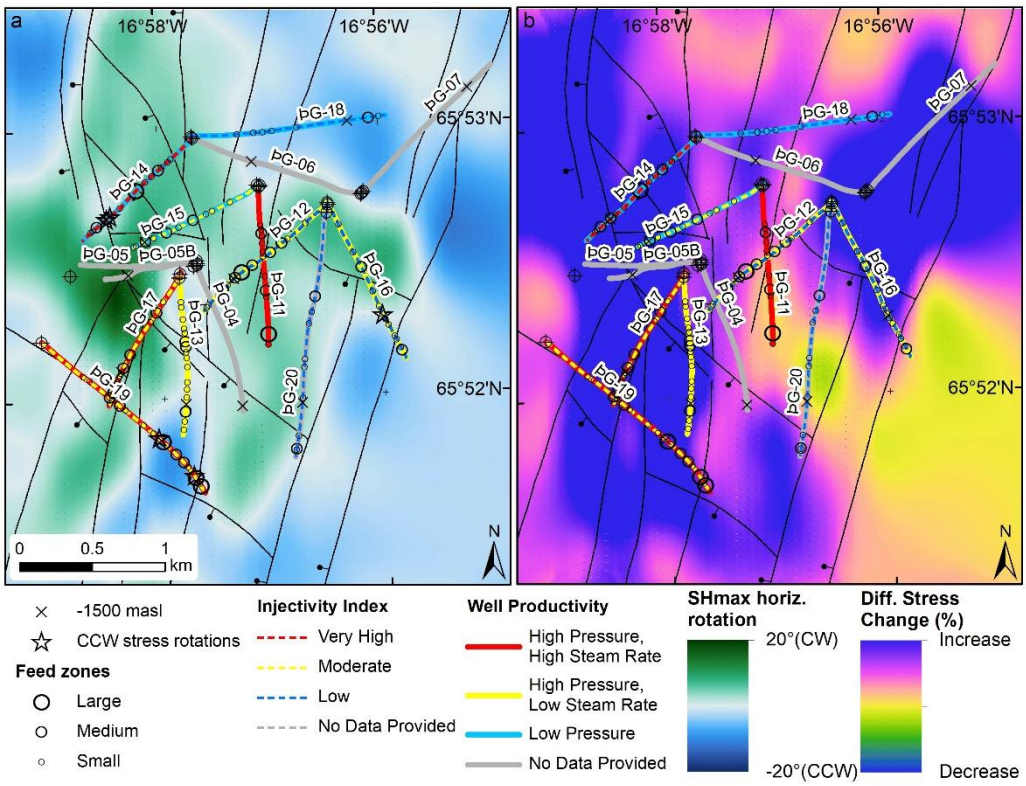


Figure 4. a) Horizontal axis rotation in SHmax. b) Percent change in differential stress

3.2.2 Differential Stress Change

In addition to stress rotations, the fault slip also causes increases in differential stress (magnitude of the maximum stress minus magnitude of the minimum stress) throughout the reservoir (Figure 4b). An increase in differential stress increases the likelihood that a fault will slip and possibly generate or maintain permeability by remaining open due rugosity/sinuosity or asperities along the fault plane(s). The increase in differential stress is largest along the western margin of the field, collocated with the oppositely dipping normal faults that make up the accommodation zone. Of the most productive wells (high pressure, high steam rate and high pressure, low steam rate and high injectivity index) all but ÞG-11 are located in areas of relatively high differential stress change at reservoir depth.

3.2.3 Coulomb Shear Traction Change and Dilation

The fault slip causes increases in both the Coulomb shear traction on faults/fractures and dilation (and locally minor shortening) throughout the model domain. Increases in Coulomb shear traction, which incorporates changes in shear stress relative to changes in normal stress, increases the likelihood that a fault will slip and possibly generate or maintain permeability by remaining open due to rugosity/sinuosity or asperities along the fault plane. The largest magnitude increases in Coulomb shear traction are focused along the western and northern parts of the well field, whereas Coulomb shear traction increases are relatively minor in the southeastern part of the well field. Dilation is the opening component of strain, a situation in which generation and maintenance of permeability would be expected if the fracture remains propped open. Similar to Coulomb shear traction, the highest magnitude dilation occurs along the western and northern parts of the well field, whereas low strain and locally minor shortening occur in the southeastern part of the well field.

The most productive wells (high pressure/high steam rate, high pressure/low steam rate, and high injectivity index) are mostly located in areas of moderate to high increases in shear traction and high magnitude dilation at reservoir depth. The exceptions to this are ÞG-11, which is one of the most productive wells in the field, and ÞG-12 both of which are located in areas of only moderate shear traction increase and moderate dilation. Three low pressure wells (ÞG-14, ÞG-15, and ÞG-18) are also located in areas of high increases in Coulomb shear traction. Though ÞG-15, and ÞG-18 are relatively low productivity wells, ÞG-14 has the highest injectivity index of wells examined in this study.

4 DISCUSSION

We conclude that there are two primary controls on permeability distribution in the Þeistareykir geothermal field; lithologic and structural. The lithologic control is related to the occurrence of hard basaltic formations at depth and importantly, silicic intrusive rocks. The silicic rocks occur most prevalently in the southern and western most wells, ÞG-19, ÞG-17, ÞG-14, ÞG-13. Though many NNW-striking (rift-parallel) faults appear to contribute to permeability throughout the field, the 'sweet spot' is intimately linked to the accommodation zone between west-dipping faults to the north and east-dipping faults to the south along the western side of the wellfield. The accommodation zone controls the largest magnitude changes in the stress field (both azimuths and magnitudes), dilation, and changes to resolved stresses on fault and fracture surfaces throughout the wellfield and the surrounding area. The stress rotations are particularly interesting. The BHI data display counter-clockwise SHmax rotations of ~2-22° at reservoir depths in all three wells analyzed (ÞG-14, ÞG-16, and ÞG-19). In each case, the counter-clockwise SHmax rotations are collocated with large and medium feed zones in all three wells (Wallis et al., 2026). Coupled with the fact that ÞG-14, ÞG-16, and ÞG-19 span the northern, western, and eastern parts of the wellfield, this may indicate that in addition to ÞG-14, ÞG-16, and ÞG-19, counter-clockwise stress rotations may be associated with productive feed zones throughout the geothermal reservoir. The dynamic modeling results demonstrate that the areas around ÞG-14, ÞG-16, and ÞG-19 all are associated with counter-clockwise stress rotations (Figure 4). Similarly, vertical axis stress rotations have been documented in areas of structural complexity worldwide (Fodor, 2007, Hardebeck and Okada, 2018) and are associated with productive permeability (Fercho, 2020). Vertical axis stress rotations may be a controlling mechanism for why permeability tends to occur in areas of structural complexity like accommodation zones, fault step-overs, displacement transfer zones, pull-aparts and fault terminations (Curewitz and Karson, 1997, Wilson and Rowland, 2016, Wallis et al., 2018 & 2023, Faulds et al., 2021, Siler et al., 2023).

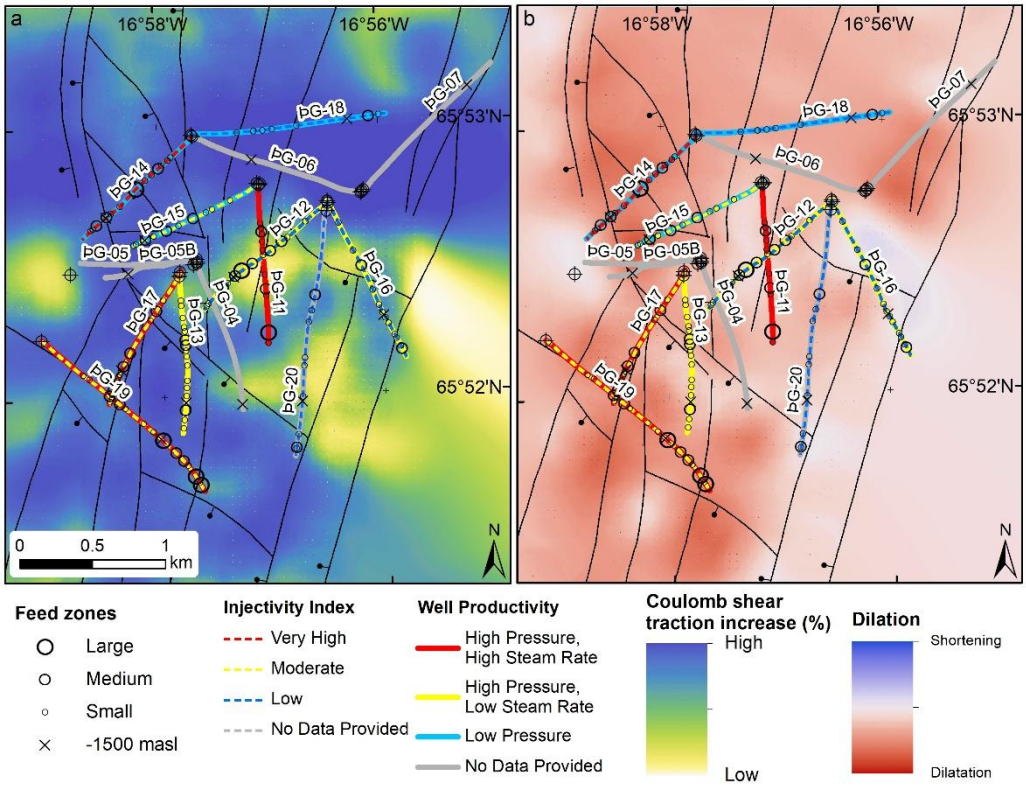


Figure 5. a) Percent increase in Coulomb shear traction. b) Dilation vs. shortening

High values in the other proxies for permeability generation and maintenance examined herein; differential stress change, coulomb shear traction change, and dilation are all spatially associated with many of the most permeable wells in the field, wells with high injectivity, high pressure, or both. These wells predominantly lie along the western side of the field in the accommodation zone.

Interestingly, one of the most productive wells in the field, ÞG-11, lies in a location expected to have clockwise stress rotation, minor increases in differential stress, and relatively low dilation. We propose two possible explanations for this. Firstly, it is possible that the generalized fault model does not adequately capture the fault structure in the area near ÞG-11. The accommodation zone may, for instance, extend farther to the east than the generalized fault model indicates. In addition, the exclusively steep fault dips employed in the modelling, which are inconsistent with the range of fracture dips in the BHI data, may play a role as well. Secondly, the permeability in ÞG-11 may be related to characteristics that are not well captured by the dynamic modeling. ÞG-11 has one large feed zone near the bottom of the well. This feed zone, for instance, may be associated with one or a small number of large aperture fractures not captured by the 50 m discretization of the model domain.

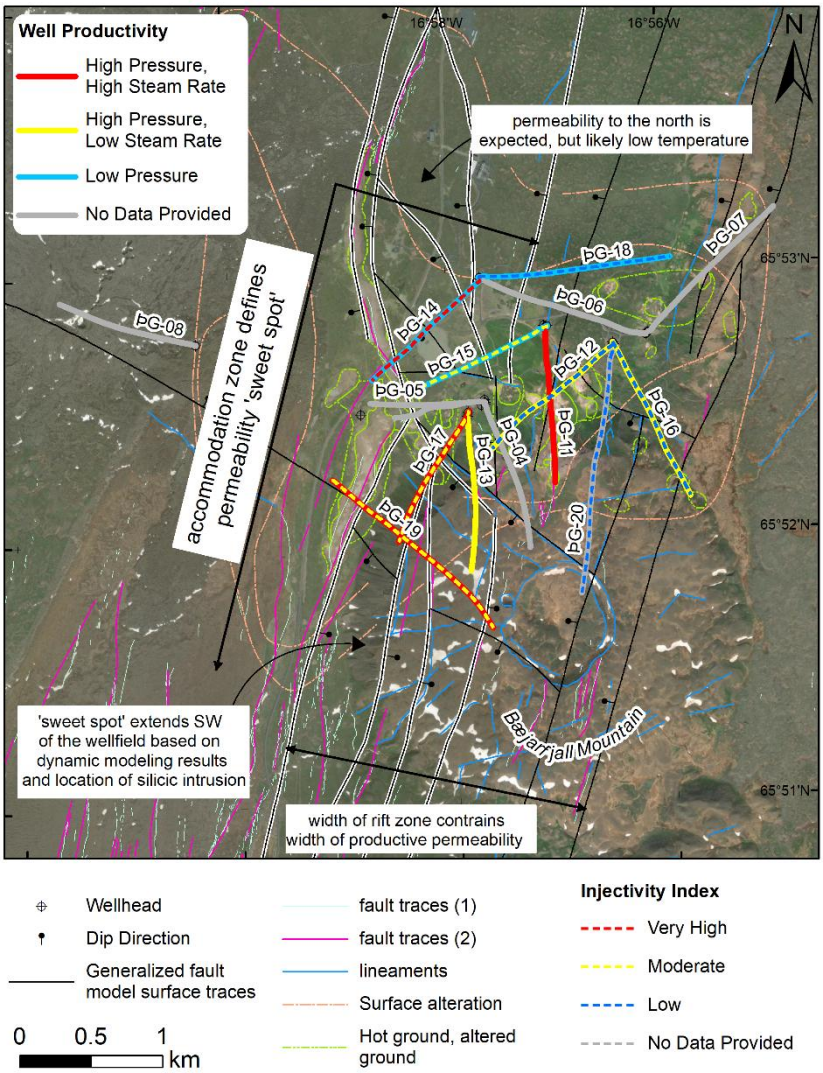


Figure 6. Map illustrating the permeability results of this and its companion study (Wallis et al., 2026). Well productivity is shown as a thick, solid well path line beneath a dotted line for injectivity index. The faults that constitute the accommodation zone are highlighted in white.

Still, the dynamic modeling results are largely consistent with the well productivity and injectivity index results. Figure 6 illustrates the control on permeability throughout the well field as indicated by this study. The ~2 km-wide rift zone constrains the width of productive permeability, within which the NNW-striking (rift zone parallel) normal faults are the predominant permeability control. The 'sweet spot' of productive permeability occurs within the western ~1/2 of the rift zone, where west-dipping faults to the north and east-dipping faults to the south constitute an accommodation zone. The northern-end of the accommodation zone, though permeable, is

relatively lower temperature, as evidenced by the very permeable, but lower temperature, lower pressure well ÞG-14. On the other hand, the southern end of the accommodation zone is spatially coincident with the silicic intrusive rocks, meaning that this part of the field is expected to display both the key lithological and structural controls on permeability.

CONCLUSIONS

A reservoir-scale geomechanical study on the controls of permeability at Þeistareykir geothermal field is presented. This work was conducted in concert with a wellbore-scale geomechanical study (Wallis et al., 2026, this volume). Together these two papers represent a novel, multi-scale geomechanical analysis conducted in order to inform on the controls of geothermal reservoir permeability. Counter-clockwise, vertical axis stress rotations are seen at both scales and are inferred to by a key control on permeability. Vertical axis stress rotation localized in areas of structural complexity, like the accommodation zone at Þeistareykir, may explain why areas of structural complexity (e.g., accommodation zones, fault step-overs, displacement transfer zones, pull-aparts, and fault terminations) commonly host geothermal systems worldwide.

Based on the results present herein we demarcate a 'sweet spot' where the key lithologic and structural permeability controls are most prevalent. This area is relatively long (NNE/SSW) and narrow (WNW/SSE) parallel to predominant rift parallel structure. This geometry is controlled by the center of the accommodation zone located at the NW corner Bæjarfjall Mountain, and the high values for the various permeability proxies established via dynamic modelling, which extend to the north and south of the accommodation zone.

Acknowledgements

We would like to thank Landsvirkjun for supporting this work and granting permission to publish the results.

REFERENCES

Bergerat, F., Angelier, J. and Homberg, C., 2000. Tectonic analysis of the Husavik-Flatey Fault (northern Iceland) and mechanisms of an oceanic transform zone, the Tjörnes Fracture Zone. Tectonics, 19(6), pp.1161-1177.

Blischke, A., Hjartardóttir, Á. R., Guðnason, E. Á., Ágústsdóttir, Þ., Vilhjálmsson, A. M., Óladóttir, A. A., Benediktsdóttir, Á. and Egilson, Þ. (2022). The Þeistareykir Geothermal Field: Structural Field Assessment and Compartmentalisation. Iceland GeoSurvey, ÍSOR-22039, short report, 26 p.

Curewitz, D. and Karson, J.A., 1997. Structural settings of hydrothermal outflow: fracture permeability maintained by fault propagation and interaction. Journal of Volcanology and Geothermal Research, 79, 149–168, https://doi.org/10.1016/S0377-0273(97)00027-9.

Faulds, J.E., Coolbaugh, M.F. and Hinz, N.H. 2021. Inventory of Structural Settings for Active Geothermal Systems and Late Miocene (c. 8 Ma) to Quaternary Epithermal Mineral Deposits in the Basin and Range Province of Nevada. Nevada Bureau of Mines and Geology Report 58, 3 plates, scale 1:2,500,000.

Faulds, J.E., Varga, R.J., 1998. The role of accommodation zones and transfer zones in the regional segmentation of extended terranes. Special papers-Geological Society of America, pp.1-46.

Fercho, S., Hinz, N., Casteel, J., Turk, J., 2020. Analysis of Natural and Drilling Induced Fractures from Newly Acquired Borehole Image Logs at the Star Peak Geothermal Field, NV: Implications for Localized Stress Field Rotation Within a Normal Fault Step-Over. Geothermal Resources Council Transactions, 44.

Fodor, L.I., 2007. Segment Linkage and the State of Stress in Transtensional Transfer Zones: Field Examples From The Pannonian Basin. Geological Society, London, Spec. Pub, v. 290, 417-431.

Hardebeck, J. L., and Okada, T., 2018. Temporal Stress Changes Caused By Earthquakes: A review. Journal of Geophysical Research: Solid Earth, 123, 1350–1365.

Khodayar, M. and Björnsson, S., 2018. Structures and styles of deformation in rift, ridge, transform zone, oblique rift and a microplate offshore/onshore North Iceland. International Journal of Geosciences, 9(8), pp.461-511.

Khodayar, M., Björnsson, S., Kristinsson, S.G., Karlsdóttir, R., Ólafsson, M. and Víkingsson, S., 2018. Tectonic control of the Theistareykir geothermal field by rift and transform zones in North Iceland: A multidisciplinary approach. Open Journal of Geology, 8(6), pp.543-584.

Khodayar, M., Björnsson, S., Kristinsson, S.G., Karlsdóttir, Ágústsson, K., and R., Ólafsson, M., 2015. Tectonic Control of Alteration, Gases, Resistivity, Magnetics and Gravity in Þeistareykir Area. Implications for Northern Rift Zone and Tjörnes Fracture Zone. Iceland GeoSurvey (ÍSOR) Report LV-2015-039.

Magnúsdóttir, S. and Brandsdóttir, B., 2011. Tectonics of the Þeistareykir fissure swarm. Jökull, 61, pp.65-79.

Sæmundsson, K., 2007. Geology of Þeistareykir (in Icelandic). Iceland GeoSurvey, Short Report ÍSOR-07270, 23 p.

Sæmundsson, K., Hjartarson, Á., Kaldal, I., Sigurgeirsson, M. Á., Kristinsson, S. G., and Víkingsson, S., 2012. Geological Map of Northern Volcanic Zone, Iceland. Northern part. 1:100.000. Reykjavík, Iceland GeoSurvey and Landsvirkjun.

Siler, D.L., 2023. Structural discontinuities and their control on hydrothermal systems in the Great Basin, USA. Geoenergy, 10 pp. https://doi.org/10.1144/geoenergy2023-009.

Tibaldi, A., Corti, N., Bonali, F.L., Mariotto, F.P. and Russo, E., 2020. Along-rift propagation of Pleistocene-Holocene faults from a central volcano. Journal of Structural Geology, 141, p.104201.

Þorsteinsdóttir, U., Einarsson, G.M., Gautason, B., Sigurgeirsson, M.A., Blischke, A. and St. Ásgeirsdóttir, R., 2019. Þeistareykir Geothermal Field. A Structural Model. Report LV-2019-044, ÍSOR-2019/040, 44 pp.

Wallis, I.C., Rowland, J.V. and Dempsey, D. 2018. The relationship between geothermal fluid flow and geological context: a global review. Geothermal Resources Council Transactions, 42.

Wallis, I.C., Rowland, J.V., and Dempsey, D.E. 2023. Geologic Controls on Geothermal System Location and Type. Transactions, New Zealand Geothermal Workshop.

Wallis, I.C., Siler, D.L., Mortensen, A.K., and Egertsson, G.H., 2026. Stress, Slip, and Productivity: Integrated Geomechanical Modeling of the Þeistareykir Geothermal Reservoir – Part 1 Wellbore Scale. Proceedings World Geothermal Congress 2026, this volume.

Wilson, C.J.N. and Rowland, J.V., 2016. The volcanic, magmatic and tectonic setting of the Taupo Volcanic Zone, New Zealand, reviewed from a geothermal perspective. Geothermics, 59, 168–187, https://doi.org/10.1016/j.geothermics.2015.06.013.